Charge-ordering modulation observed in the $(La_{0.5}Mn_{0.5})MnO_3$ phase of the multiphased manganite $La_{0.9}Sn_{0.1}MnO_3$ at room temperature

Y. Q. Wang[a] and X. F. Duan
Beijing Laboratory of Electron Micoscopy, Center for Condensed Matter Physics and Institute of Physics, Chinese Academy of Sciences, P.O. Box 2724, Beijing 100080, China

Z. H. Wang, J. R. Sun, and B. G. Shen
State Key Laboratory of Magnetism, Institute of Physics and Center for Condensed Matter Physics, Chinese Academy of Sciences, Beijing, 100080, China

(Received 27 December 2000; accepted for publication 27 February 2001)

At room temperature, the lattice image of a modulated structure associated with charge ordering has been observed in the $(La_{0.5}Mn_{0.5})MnO_3$ phase of $La_{0.9}Sn_{0.1}MnO_3$, which is composed of two-type phases: ABO_3 and $A_2B_2O_7$. Results of electron energy loss spectroscopy and energy dispersive x-ray spectroscopy show that the need of the chemical balance and small A-site radius for the $(La_{0.5}Mn_{0.5})MnO_3$ phase are the main reasons for the appearance of charge ordering stripes. © *2001 American Institute of Physics.* [DOI: 10.1063/1.1368183]

Studying the charge-ordering (CO) phenomena in the ABO_3-type rare earth manganites with the formula, $Ln_{1-x}A_xMnO_3$, is particularly fascinating, since they are associated with the magnetotransport properties that are sensitive to electronic and geometric factors. CO in the manganites has become the topic of extensive studies recently,[1–7] although it was noticed by Wollan and Kochler[8] in 1955, and later by Jirak *et al.*[9] in 1985. Recently, the modulated structures in $La_{1-x}Ca_xMnO_3$ ($x=0.5$, 0.67, 0.75) have been successfully explained in terms of Mn^{3+}–Mn^{4+} ordering and the d_{z^2} orbital ordering of Mn^{3+}.[4–7] Previously, it was proposed that the cell doubling along the **a**-axis could be achieved by the orientational ordering of d_{z^2} orbitals in Mn^{3+}, in addition to the Mn^{3+}–Mn^{4+} ionic ordering.[10,11] The investigation of the charge-ordered state in manganites showed that average radius of the A-site cations was one of the important factors influencing the properties of the manganites.[12,13] The manganites exist in a wide variety of crystal forms, so the effect of lattice structure and dimensionality on the formation of charge-ordering stripes and their properties should be studied in detail.

In this letter, we reported high-resolution transmission electron microscopy (HRTEM) studies of $La_{0.9}Sn_{0.1}MnO_3$, concentrating on the observation of the modulated structures in the ABO_3 phase due to charge-ordering transition. Stripes associated with CO were observed in the ABO_3 phase at room temperature.

Polycrystalline samples with a nominal composition of $La_{0.9}Sn_{0.1}MnO_3$ were synthesized by the conventional solid-state reaction from La_2O_3, SnO_2, and MnO_2. The specimens for transmission electron microscopy were prepared by mechanical polishing followed by ion milling. A Philips CM200-FEG transmission electron microscope equipped with a charge coupled device array detector and Gatan imaging filter system was used for high-resolution electron microscopy (HREM) imaging, diffraction, and electron energy-loss spectroscopy (EELS) analyses. The point to point resolution was 2.4 Å. Local composition measurements were undertaken in JEM 2000-FX using quantitative energy dispersive x-ray spectroscopy (EDS) with a spot size of about 20 nm.

According to the x-ray diffraction (XRD) pattern of $La_{0.9}Sn_{0.1}MnO_3$, the XRD lines can be divided into two sets. One set can be indexed with the orthorhombic crystal structure $a \approx b = 5.5$ Å, $c = 7.7$ Å identified as the ABO_3 phase. The other can be indexed with the pyrochlore structure characterized by $A_2B_2O_7$ phase. The sample $La_{0.9}Sn_{0.1}MnO_3$ is thus composed of two-type phases: ABO_3 and $A_2B_2O_7$. EELS and EDS were used for the composition analyses of the different phases in the sample. At the same time, the electron diffraction studies of the different areas were carried out. It confirms that two ABO_3 phases and two $A_2B_2O_7$ phases coexist in the sample, and the former is the dominant phase (80% of the total in volume). The chemical formula of the two $A_2B_2O_7$ phases are: $(Sn_{0.4}Mn_{0.6})_2Mn_2O_7$ and $(La_{0.8}Mn_{0.2})_2Sn_2O_7$, respectively. More detailed structural studies of the two $A_2B_2O_7$ phases will be discussed elsewhere. There are two main phases in the ABO_3 phase, with the chemical formula of $La_{0.9}MnO_3$ and $(La_{0.5}Mn_{0.5})MnO_3$, respectively. Both phases have a similar volume fraction (40% of the total). Further studies using HRTEM show that there is one kind of modulated structure associated with CO in the paramagnetic state of the $(La_{0.5}Mn_{0.5})MnO_3$ phase.

The $[0\,0\,1]_0$ zone-axis HREM image recorded from the ABO_3 phase at room temperature is shown in Fig. 1. It can be seen from this image that there is evident modulated structure. The modulated structure is along the $[2\,0\,0]_0$ direction with the periodicity of about 11.6 Å. The image in Fig. 1 is consistent with the model proposed by Mori *et al.*[7] for $La_{0.5}Ca_{0.5}MnO_3$. The enhanced contrast of the dark fringes can also been explained by the strain induced by the Jahn–Teller distortion of the $Mn^{3+}O_6$ octahedra. The dark fringes are composed of ~ 2.78 Å distorted square grids. X-ray diffraction and neutron scattering measurements indicated that the polarization of the modulated wave (resulting

[a]Author to whom correspondence should be addressed; electronic mail address: yiqianwang@usa.net

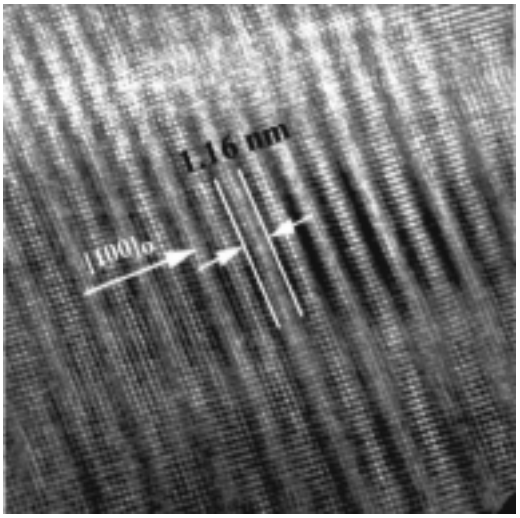

FIG. 1. $[0\,0\,1]_0$ zone-axis HREM image showing the charge ordering stripes with modulation periodicity of 11.6 Å and direction along $[2\,0\,0]_0$ in orthorhombic crystal structure, which is recorded from ABO_3 phase of the composite $La_{0.9}Sn_{0.1}MnO_3$ at room temperature.

from the ionic ordering of Mn^{3+} and Mn^{4+}) is along the **a**-axis direction and involves the movements of cations as well as oxygen.[14] This can also be seen from Fig. 1. It should be noted that the area of this phase is so small ($\sim$20 nm) that the selected area diffraction pattern is very difficult to obtain.

In order to further clarify the appearance of the modulated structure in the ABO_3 phase, EELS and EDS analyses are carried out. EELS and EDS for the same areas (showing the charge ordering stripes) of the ABO_3 phase are shown in Fig. 2. From the analyses of Fig. 2(a), it can be seen that the peak at 532 eV corresponds to the O *K* edge; the peak at 640 eV corresponds to the $L_{2,3}$ edges of Mn; the peak at 830 eV corresponds to $M_{4,5}$ edges of La. The quantification of the EELS spectra shows that Mn:O$\approx$1:2. It is very difficult to get an accurate quantification of La and Mn. The quantification of EDS spectra [Fig. 2(b)] for the same area studied by EELS indicates that La:Mn$\approx$1:3. So the chemical formula of the area is proposed as $(La_{0.5}Mn_{0.5})MnO_3$ by combining the results of EELS and EDS. The doped Sn in this phase is so little in this area that EELS and EDS cannot detect its existence. From the analyses of the chemical balance and composition, the Mn ions in the A site should be $+2$ in valence in order to reduce elastic energy. The effective radius of nine-fold coordination Mn^{2+} is about 1.04 Å[15] which is similar to that of Ca^{2+} (1.18 Å). It can reduce the elastic energy of the lattice and increase the stability of the structure. The valence of Mn ion in B site is equal to 3.5 according to the rule of chemical balance. This also means that there exist equal amounts of Mn^{3+} and Mn^{4+} in this phase. The Mn^{3+} is subjected to a Jahn–Teller deformation, which produces a deformed MnO_6 octahedron. The elastic interaction between deformed octahedra may lead to a cooperative Jahn–Teller effect in order to minimize the total free energy of elastic origin. From the results of EELS and EDS, it is more reasonable to explain the HREM image in terms of the CO of Mn^{3+} and Mn^{4+}.

Arulraj *et al.*[12] studied the nature of the CO in $Y_{0.5}Ca_{0.5}MnO_3$ with a very small average radius of A-site cations. They found that the occurrence of CO in the paramagnetic state, at relatively high temperature of about 260 K. Their studies indicated that the nature of the charge ordering in $Y_{0.5}Ca_{0.5}MnO_3$ which was dominated by the cooperative Jahn–Teller effect and the associated lattice distortion was distinct from the analogous manganites with larger average radius of A-site cations. They[13] also systematically studied the extraordinary sensitivity of charge ordering to the average radius of A-site cations. They suggested that the competition between the covalent mixing of the oxygen O: 2*p* orbital with A-site and B-site cation orbitals plays a crucial role and that the strain effects due to size mismatch between A-site cations can also cause considerable changes in the temperature for CO transition T_{CO}. Their results[13] indicated that the T_{CO} increases with decreasing average radius of A-site cations. In the present case, the tolerance factor is less than that for $Sm_{0.5}Ca_{0.5}MnO_3$, the T_{CO} of which is about 280 K.[16] Therefore, it is reasonable to observe the earlier CO phenomenon at room temperature.

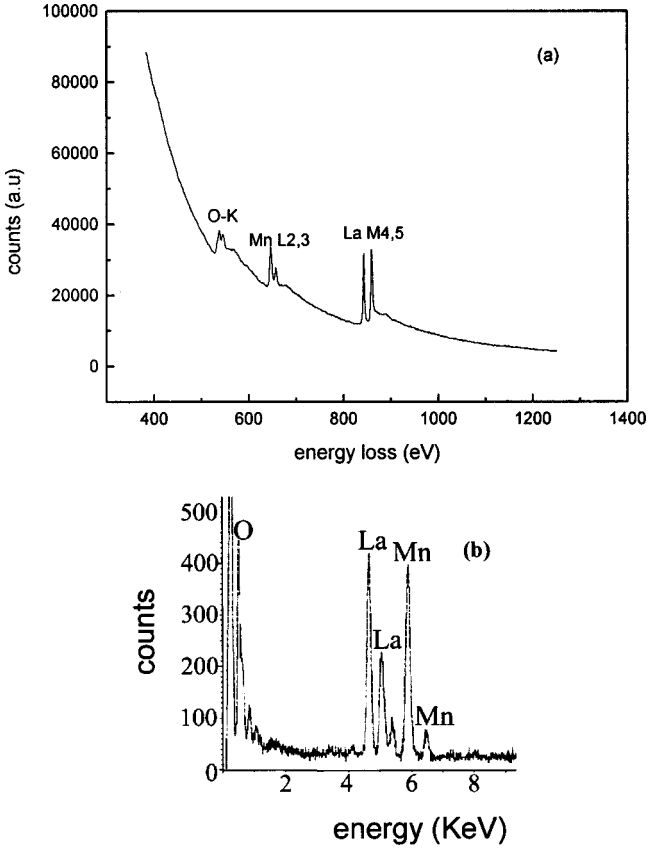

FIG. 2. (a) EELS and (b) EDS spectra of the same area in ABO_3 phase corresponding to the region in Fig. 1.

In conclusion, one structural modulation has been found in the $(La_{0.5}Mn_{0.5})MnO_3$ phase of the multiphased manganite $La_{0.9}Sn_{0.1}MnO_3$. The modulation can be explained in terms of CO. The CO phases have unusual properties, especially the lattice responses. CO phenomenon occurring at room temperature may provide a clue to interpret the unsolved problems existing in colossal magnetoresistance (CMR) effect and the mechanism of CMR.

The authors would like to acknowledge the support of China NSF outstanding Young Scientist Grant (B-class, No. 59825503) and thank Professor K. H. Kuo for encouragement. Authors from the State Key Laboratory of Magnetism

also thank the financial support of the State Key Project for Basic Research of China.

[1] Y. Tomioka, A. Asamitsu, Y. Moritomo, H. Kuwahara, and Y. Tokura, Phys. Rev. Lett. **74**, 5108 (1995).
[2] V. Kiryukhin, D. Casa, J. P. Hill, B. Keimer, A. Vigliante, and Y. Tokura, Nature (London) **386**, 813 (1997).
[3] Y. Moritomo, H. Kuwahara, Y. Tomioka, and Y. Tokura, Phys. Rev. B **55**, 7549 (1997).
[4] A. P. Ramirez, P. Schiffer, S.-W. Cheong, C. H. Chen, W. Bao, T. T. M. Palstra, P. L. Gammel, D. J. Bishop, and B. Zegarski, Phys. Rev. Lett. **76**, 3188 (1996).
[5] C. H. Chen, S.-W. Cheong, and H. Hwang, J. Appl. Phys. **81**, 4326 (1997).
[6] C. H. Chen and S.-W. Cheong, Phys. Rev. Lett. **76**, 4042 (1996).
[7] S. Mori, C. H. Chen, and S.-W. Cheong, Nature (London) **392**, 473 (1998).
[8] E. O. Wollan and W. C. Koehler, Phys. Rev. **100**, 545 (1955).
[9] Z. Jirak, S. Krupicka, Z. Simsa, M. Dlouha, and S. Vratislav, J. Magn. Magn. Mater. **53**, 153 (1985).
[10] J. B. Goodenough, Phys. Rev. **100**, 564 (1955).
[11] E. Pollert, S. Krupicka, and E. Kuzmicova, J. Phys. Chem. Solids **43**, 1137 (1982).
[12] A. Arulraj, R. Gundakaram, A. Biswas, N. Gayathri, A. K. Raychaudhuri, and C. N. Rao, J. Phys.: Condens. Matter **10**, 4447 (1998).
[13] A. Arulraj, P. N. Santhosh, R. S. Gopalan, A. Guha, A. K. Raychaudhuri, N. Kumar, and C. N. Rao, J. Phys.: Condens. Matter **10**, 8497 (1998).
[14] P. G. Radaelli D. E. Cox, M. Marezio, and S.-W Cheong, Phys. Rev. B **55**, 3015 (1997).
[15] R. D. Shannon, Acta Crystallogr., Sect. A: Cryst. Phys., Diffr., Theor. Gen. Crystallogr. **38632**, 751 (1976).
[16] Y. Moritomo, A. Machida, S. Mori, N. Yamamoto, and A. Nakamura, Phys. Rev. B **60**, 9220 (1999).